

3.3A AN EVALUATION OF THE ACCURACY OF SOME RADAR WIND PROFILING TECHNIQUES

A. J. Koscielny and R. J. Doviak

National Severe Storms Laboratory
1313 Halley Circle
Norman, OK 73069

INTRODUCTION

Major advances in Doppler radar measurement in optically clear air have made it feasible to monitor radial velocities in the troposphere and lower stratosphere. For most applications we want to monitor the three dimensional wind vector rather than the radial velocity. Measurement of the wind vector with a single radar can be made assuming a spatially linear, time invariant wind field. The components and derivatives of the wind are estimated by the parameters of a linear regression of the radial velocities on functions of their spatial locations. The accuracy of the wind measurement thus depends on the locations of the radial velocities.

PETERSON and BALSLEY (1979) point out that a tradeoff exists for a given technique between the accuracies of horizontal and vertical component measurements. Because we usually need to measure the three components of wind with different accuracy and as inexpensively as possible, we are led to evaluate the suitability of some of the common retrieval techniques for simultaneous measurement of both the vertical and horizontal wind components. The techniques we will consider are fixed beam, azimuthal scanning (VAD) and elevation scanning (VED).

ERROR ANALYSIS THEORY

The estimation of the parameters of a linear wind field from radial velocities is discussed by KOSCIELNY et al. (1982). The measured radial velocity v_r can be modelled by a linear regression equation of the form

$$v_r = P_m K_m + \epsilon \quad (1)$$

where P_m is a row vector of regressor variables which are functions of range r , azimuth θ , and elevation angle θ_e ; K_m is a column vector of m parameters. The measured v_r , a reflectivity weighted mean of radial velocities within the radar's resolution volume, can contain errors ϵ due to nonuniform reflectivity, turbulence, targets such as hydrometeors that move relative to the wind, and a nonlinear wind. It can be shown that, given n measurements of v_r , least squares estimates of K_m are computed by

$$\hat{K}_m = (P_{nm}^T P_{nm})^{-1} (P_{nm}^T V_n) \quad (2)$$

where T indicates transpose and P_{nm} is an $n \times m$ matrix of the regressor variables corresponding to the n radial velocity measurements in V_n . Measurement errors in the radial velocities produce uncertainties in the estimate K_m and the covariances of K_m about K_m are given by

$$C_{mm} = (P_{nm}^T P_{nm})^{-1} \sigma_\epsilon^2 \quad (3)$$

where σ_ϵ^2 is the variance of ϵ .

If the wind field has variations not modeled by (1), the \hat{K}_m will be biased and the amount of bias B_m is given by the product of a known alias matrix $A_{m\ell}$ with the vector K_ℓ of the ℓ unknown parameters of the wind field not included in K_m . Thus

$$B_m = A_{m\ell} K_\ell \quad (4)$$

where

$$A_{m\ell} = (P_{nm}^T P_{nm})^{-1} (P_{nm}^T P_{n\ell}). \quad (5)$$

$P_{n\ell}$ is a matrix of regressor variables for the components not included in (1).

The various techniques referred to in the introduction assume the wind to be uniform (i.e., the first and higher order derivatives are zero) over the data analysis volume. However, because w cannot be uniform for any appreciable depth of the troposphere (i.e., w must be zero at the earth's surface), the horizontal wind can never be uniform at all heights. Thus we must account for errors produced by wind shear. We propose to analyze the errors in these techniques by computing the bias and variance of the least squares estimates \hat{K}_m with assumptions that σ_ϵ^2 is constant and the wind field is actually linear. Thus K_3 contains the three uniform components u_0, v_0, w_0 and K_8 contains the 8 spatial derivatives ($u_x, u_z, v_y, v_z, u_y + v_x, w_x, w_y, w_z$) of the linear wind. In our evaluation and comparison of techniques, we assume that a total of n measurements are available for each and these n measurements are distributed in space to estimate wind at some height h .

(a) Fixed Beam

We consider a configuration for the fixed beam technique in which three beams, one vertical and two off-vertical at elevation θ_e , are sampled. The off-vertical beams usually have perpendicular horizontal projections; for convenience, we will consider them to have azimuths 0° and 90° . The total number of radial velocity measurements for a height h for all three beams is n ; for generality, we let the number of vertical measurements be N .

The bias and variance properties of the estimates $\hat{K}_3^T = (u_0, v_0, w_0)$ are computed in Appendix 1 using (3) and (5), and we find that, for $n = 3N$,

$$\begin{aligned} \text{VAR}(\hat{u}_0) &= \text{VAR}(\hat{v}_0) = \frac{\sigma_\epsilon^2}{n} \cdot 3 \cdot (\sec^2 \theta_e + \tan^2 \theta_e) \\ \text{VAR}(\hat{w}_0) &= \frac{\sigma_\epsilon^2}{n} \cdot 3 \end{aligned} \quad (6)$$

$$\text{Bias} \begin{bmatrix} \hat{u}_0 \\ \hat{v}_0 \\ \hat{w}_0 \end{bmatrix} \approx h \begin{bmatrix} u_x \cot \theta_e + w_x \\ v_y \cot \theta_e + w_y \\ 0 \end{bmatrix} \quad (7)$$

The bias equation is approximate because we have used $h \approx r \sin \theta_e$ which should be appropriate for $r \leq 30$ km. From (7) we see that the bias due to spatial derivatives is a linear function of height which is expected because the beam separation is linearly dependent on h . In addition, we see from (6) and (7)

that the variance decreases with n , but that the bias cannot be reduced by data averaging.

(b) Azimuthal Scanning

In an azimuthal scanning technique, usually called VAD (Velocity Azimuth Display), data along a circle centered on the radar are used to directly estimate the components of the uniform wind field. The results of the bias and variance equation evaluation, in Appendix 2, are that

$$\begin{aligned} \text{VAR}(\hat{u}_o) = \text{VAR}(\hat{v}_o) &= \frac{\sigma_\epsilon^2}{n} \cdot 2 \sec^2 \theta_e \\ \text{VAR}(\hat{w}_o) &= \frac{\sigma_\epsilon^2}{n} \cdot \csc^2 \theta_e \end{aligned} \quad (8)$$

$$\text{Bias} \begin{bmatrix} \hat{u}_o \\ \hat{v}_o \\ \hat{w}_o \end{bmatrix} \approx h \begin{bmatrix} w_x \\ w_y \\ 1/2(u_x + v_y) \cdot \cot^2 \theta_e \end{bmatrix} \quad (9)$$

(c) Elevation Scanning

In the elevation scanning (Velocity Elevation Display) technique, radial velocities at a height h are collected for elevation angles $\theta_o \leq \theta_e \leq 180 - \theta_o$. We assume $\frac{n}{2}$ data are collected for the two azimuths 0° and 90° so both horizontal components are measured. It is shown in Appendix 3 that

$$\begin{aligned} \text{VAR}(\hat{u}_o) = \text{VAR}(\hat{v}_o) &= \frac{\sigma_\epsilon^2}{n} \cdot \frac{4(\pi - 2\theta_o)}{\{\pi - 2\theta_o - \sin(\pi - 2\theta_o)\}} \\ \text{VAR}(\hat{w}_o) &= \frac{\sigma_\epsilon^2}{n} \cdot \frac{2(\pi - 2\theta_o)}{\{\pi - 2\theta_o + \sin(\pi - 2\theta_o)\}} \end{aligned} \quad (10)$$

$$\text{Bias} \begin{bmatrix} \hat{u}_o \\ \hat{v}_o \\ \hat{w}_o \end{bmatrix} \approx h \begin{bmatrix} w_x \\ w_y \\ (u_x + v_y) \cdot \left[\frac{\pi - 2\theta_o - \sin(\pi - 2\theta_o)}{\pi - 2\theta_o + \sin(\pi - 2\theta_o)} \right] \end{bmatrix} \quad (11)$$

ERROR COMPARISON

The results of our analysis of the three techniques, summarized in Table 1 show the variances of the wind estimates all depend on σ_ϵ^2/n . Since the variance of an average of n independent data is σ_ϵ^2/n , we will divide this quantity by the variance of the estimate of the wind component. Because of its similarity to the usual statistical definition, we term this quantity the efficiency of the estimate.

The variation of the efficiencies of the horizontal wind estimates with elevation angle are shown in Figure 1. The VAD technique has the highest efficiency of the techniques for all elevation angles. In addition, the VAD

Table 1. Variance and bias equations for horizontal and vertical wind estimates obtained from fixed beam, azimuth scanning or elevation scanning techniques. $VAR[\hat{u}_0] = VAR[\hat{v}_0]$ and for Bias (\hat{v}_0) replace x subscript with y.

	Fixed Beam (one vertical)	Azimuth Scanning (VAD)	Elevation Scanning (VED)
$VAR(\hat{u}_0)$	$\frac{\sigma_e^2}{n} 3(\sec^2\theta_e + \tan^2\theta_e)$	$\frac{\sigma_e^2}{n} 2 \sec^2\theta_e$	$\frac{\sigma_e^2}{n} 2 \left[\frac{\pi-2\theta_0}{(\pi-2\theta_0) - \sin(\pi-2\theta_0)} \right]$
$VAR(\hat{v}_0)$	$\frac{\sigma_e^2}{n} 3$	$\frac{\sigma_e^2}{n} \csc^2\theta_e$	$\frac{\sigma_e^2}{n} 2 \left[\frac{\pi-2\theta_0}{(\pi-2\theta_0) + \sin(\pi-2\theta_0)} \right]$
Bias(\hat{u}_0)	$h(u_x \cot\theta_e + w_x)$	hw_x	hw_x
Bias(\hat{v}_0)	0	$h(u_x + v_y) \frac{\cot^2\theta_e}{2}$	$h(u_x + v_y) \left[\frac{\pi-2\theta_0 - \sin(\pi-2\theta_0)}{\pi-2\theta_0 + \sin(\pi-2\theta_0)} \right]$

maintains reasonable efficiency to larger elevation angles (75°) than either fixed beam or VED.

Figure 1 shows efficiencies monotonically increasing as θ_e gets smaller. But for measurements at a constant height the range increases when θ_e decreases. Because echo power reduces in proportion to the inverse square of range (assuming the echoing layer scatters isotropically and is horizontally homogeneous) the signal-to-noise ratio (SNR) falls as θ_e decreases. If measurement errors are solely due to thermal noise and SNR is less than one, ZRNIC' (1979) shows that measurement variance σ_ϵ^2 is proportional to $(\text{SNR})^{-2}$. The effect of decreasing SNR as θ_e becomes small is to increase σ_ϵ^2 as $\csc^4 \theta_e$; the efficiency of the horizontal wind measurements thus vanishes as θ_e goes to zero. However, the variance σ_ϵ^2 includes meteorological effects such as turbulence that, in our experience, places a lower bound on σ_ϵ^2 of about $1 \text{ m}^2 \text{ s}^{-2}$. Because we are mainly concerned in this paper with elevation angles larger than 40° and, consequently, ranges less than about 30 km, σ_ϵ^2 can be regarded as a constant.

The efficiencies of the vertical velocity estimates are shown in Figure 2. The VED has the highest efficiency, but for large elevation angles the VAD is comparable. The fixed beam has a constant efficiency of $\frac{1}{3}$ since the number of vertical estimates is fixed at $\frac{n}{3}$.

The biases of the estimates show a linear dependence on the height h . To normalize bias errors, we assume $h = 1 \text{ km}$, so the bias for greater heights can be simply computed. The biases depend on the value of unknown spatial derivatives. Following WALDTEUFEL and CORBIN (1979) we use $u_x = v_y = 10^{-3} \text{ s}^{-1}$ and $w_x = w_y = 10^{-4} \text{ s}^{-1}$ as maximum values. The biases thus computed are shown in Figure 3 for the horizontal components and in Figure 4 for the vertical component. The asymmetry of the beam locations about the vertical for the fixed beam technique produces a horizontal wind bias due to u_x and v_y which decreases as $\cot \theta_e$. The horizontal wind biases for the VAD and VED are the same and are constant with elevation angle. For the fixed beam technique the vertical velocity is not biased by any derivatives. The vertical wind bias in the VED and VAD decreases with increasing elevation angle.

In conclusion, the vertical velocity variance and the bias errors can be decreased by using larger elevation angles. The variance for horizontal components increases with elevation angle but can be controlled to an extent by data averaging. Because bias increases with height, the higher altitudes may require a vertical measurement for vertical velocity.

(a) Example

The bias the variance equations can be used to choose an elevation angle for profiling. For example, suppose we wish to profile the winds at 5 km using 360 measurements with $\sigma_\epsilon = 1 \text{ m} \cdot \text{s}^{-1}$. The root mean square errors (bias squared plus variance) for the horizontal and vertical components are shown in Figures 5 and 6 for each of the techniques. We have kept vertical and horizontal errors separate because vertical velocity is much smaller and requires greater accuracy. If we require horizontal and vertical velocity accuracies of $1 \text{ m} \cdot \text{s}^{-1}$ and $0.1 \text{ m} \cdot \text{s}^{-1}$ respectively, we would use an elevation angle between 83° and 85° for the VAD and 77° and 81° for the VED. Because of the bias error, the fixed beam horizontal wind error is $1.5 \text{ m} \cdot \text{s}^{-1}$ or larger.

POSSIBLE IMPROVEMENTS

The analysis of the previous section suggests some simple improvements that can be made to increase the accuracy of the measurements.

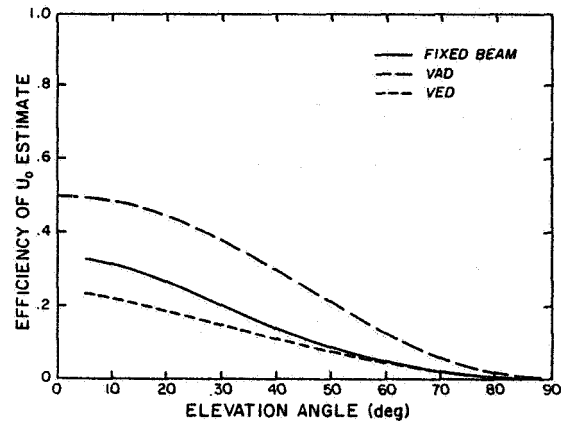


Figure 1. Variation of horizontal wind estimator efficiencies with elevation angle.

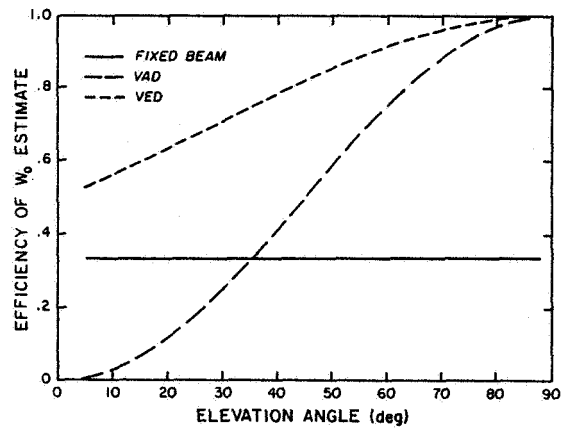


Figure 2. Variation of vertical wind estimator efficiencies with elevation angle.

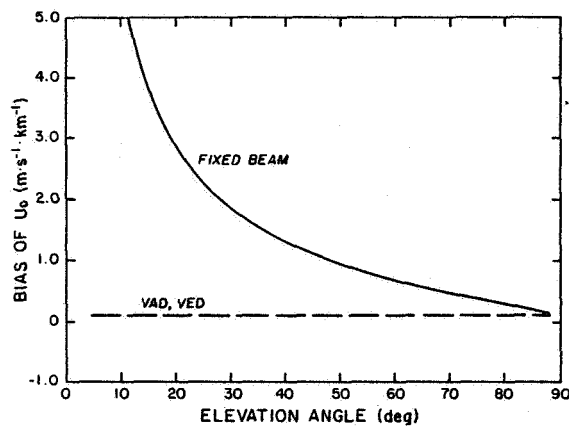


Figure 3. Bias error in horizontal wind estimator at 1 km with $u_x=v_y=10^{-3}\text{s}^{-1}$, $w_x=w_y=10^{-4}\text{s}^{-1}$. VAD and VED biases overlap.

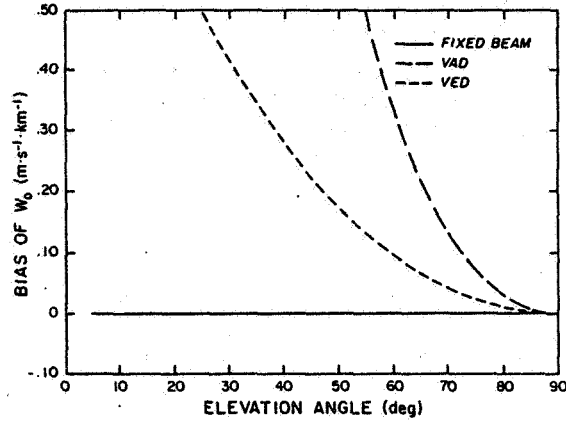


Figure 4. Bias error in vertical wind estimator at 1 km with $u_x=v_y=10^{-3}\text{s}^{-1}$, $w_x=w_y=10^{-4}\text{s}^{-1}$.

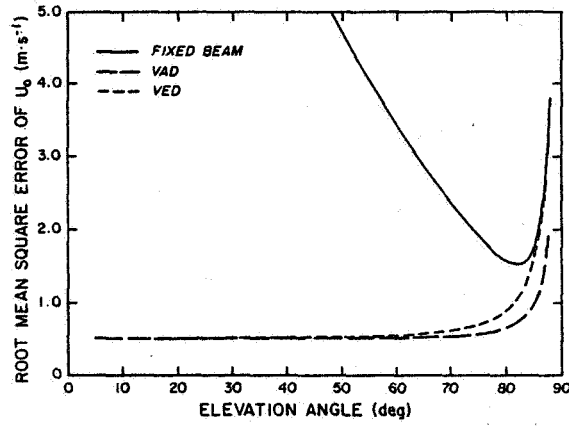


Figure 5. Root mean square error for the horizontal estimator if $\sigma=1\text{ m}\cdot\text{s}^{-1}$, $n=360$, and $h=5\text{ km}$.

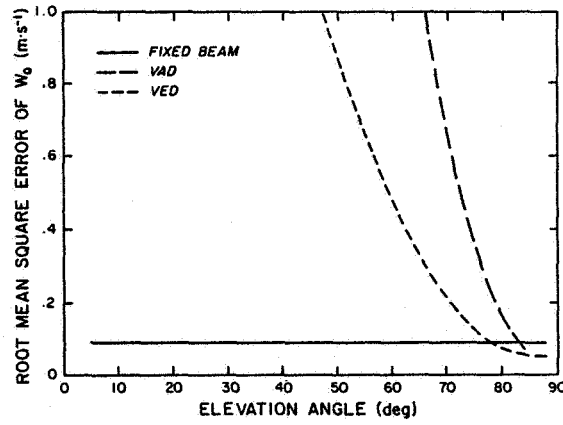


Figure 6. Root mean square error for the vertical estimator is $\sigma=1\text{ m}\cdot\text{s}^{-1}$, $n=360$, and $h=5\text{ km}$.

(a) Fixed Beam with Error Minimization

The wind estimate efficiencies for the fixed beam technique can be improved slightly by collecting a specified number N of vertical data. Minimizing the first diagonal element of the matrix in (A1.1), which is $\text{VAR}(\hat{u}_0) = \text{VAR}(\hat{v}_0)$ gives

$$\frac{N}{n} = \frac{\sin\theta_e}{\sqrt{2+\sin\theta_e}} \quad (12)$$

so N would vary from $\frac{1}{2}n$ at $\theta_e = 45^\circ$ to about $0.4n$ for θ_e near 90° . The efficiencies are shown in Figure 7 for u_0 and Figure 8 for w_0 . It can be seen that for $\theta_e > 45^\circ$, the efficiency of estimating \hat{u}_0 is unchanged but is slightly improved for w_0 .

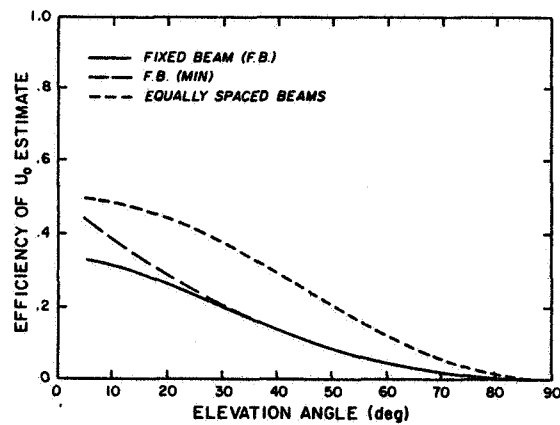


Figure 7. Horizontal wind estimator efficiency for fixed beam, fixed beam with horizontal error minimization, and fixed beam with equally spaced, off-vertical beams.

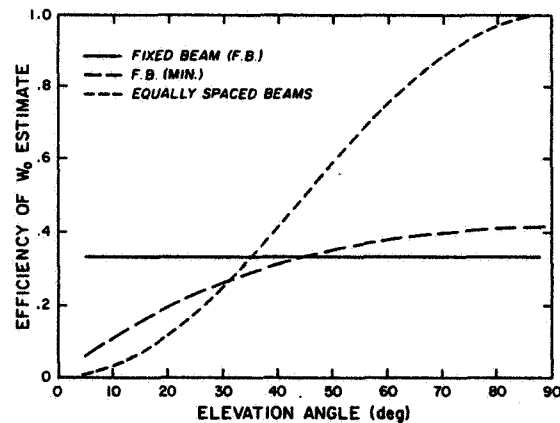


Figure 8. Vertical wind estimator efficiencies for the same techniques as described in Figure 7 caption.

The size of the variance contribution (i.e., $\sigma_e^2 \tan^2 \theta_e / N$) from the vertical velocity bias removal appears to indicate that it might be better to ignore the bias error ($w_0 \tan \theta_e$). However, for observation time intervals of several minutes, a mesoscale value of w_0 should be used. For large elevation angles, ($\theta_e > 75^\circ$) the bias error could be several meters per second or larger. For tropospheric observation under all conditions, the bias should be removed if a horizontal velocity accuracy of $1 \text{ m}\cdot\text{s}^{-1}$ is required.

(b) Three Off-Vertical Beams

For some applications, ground clutter presents a problem for vertical measurements. The fixed beam technique with three off-vertical beams with elevation θ_e and azimuths 0° , 120° , 240° is analyzed in Appendix 1b. The analysis shows that the variances (and efficiencies) of the estimates are identical to those for the VAD technique (compare Figures 1, 2 with Figures 7, 8). The biases for the u_0 estimate is very similar to the fixed beam with one vertical but the w_0 estimate is biased as shown in Figure 9.

(c) Application of the Continuity Equation to VAD Data

Vertical winds as small as few centimeters per sec are important in forecasting and, as noted earlier, w_0 should be estimated with more accuracy than the horizontal components. Because of ground clutter it may become very difficult to estimate the radial component of air motion when the beam is pointed near the vertical since the radial velocities will have values close to zero. We now show that by assuming a linear wind field and applying the mass continuity equation, we can estimate vertical wind, averaged over the circle of measurement, with the required accuracy. When mass continuity is applied, we will call the technique indirect whereas the previously discussed techniques (e.g., VAD) are direct measurements of w .

Two VAD modes in which vertical soundings can be made are fixed θ_e variable r , and variable θ_e fixed r . With variable r however, the horizontal area for which w_0 is representative varies, so we prefer the second mode. Divergence is estimated by applying Gauss's theorem to the volume V (see Figure 10) enclosed by the area S_1 at constant range from the radar and the area S_2 at constant height (DOVIK and ZRNIC', 1983). Applying mass continuity and integrating gives an areal averaged \bar{w} ,

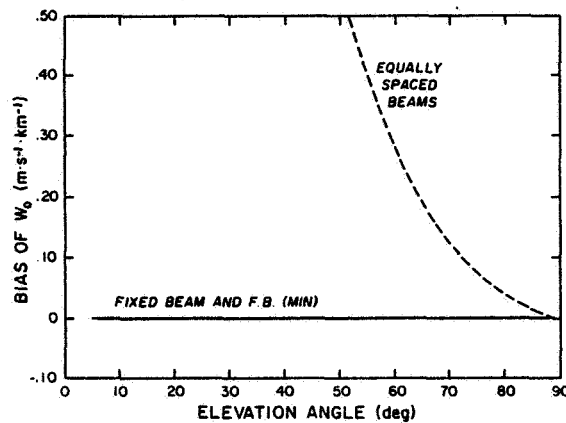


Figure 9. Vertical wind biases for the same techniques as described in Figure 7 caption.

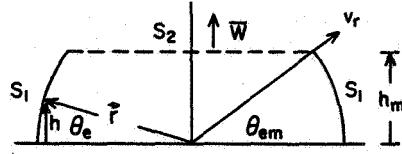


Figure 10. Geometry to estimate vertical velocity averaged over the circular area S_2 .

$$\bar{w} = \frac{-2e^{\Gamma h}}{(1-h^2/r^2)r} \int_0^h e^{-\Gamma h} C_o(h) dh \quad (13)$$

where $\Gamma = gM/RT$ is the average lapse rate of air density versus height and

$$C_o(h) = \frac{1}{2\pi r} \int_0^{2\pi} v_r r d\phi \quad (14)$$

is the average radial velocity around the circle of measurement.

To fix the number of measurements at n , we assume M values of v_r are made on each of L circles spaced at intervals Δh from $h=0$ to $h=h_m$. Then

$$\hat{C}_o(h) = \frac{1}{M} \sum_{m=1}^M \hat{v}_{rm} \quad (15)$$

If all the radial velocities are independent with the same uncertainty, then

$$\text{VAR}[\bar{w}] = \frac{4 e^{2\Gamma h} h \text{VAR}[v_r]}{r^2(1-h^2/r^2)^2 N} \frac{N}{n} \left\{ \frac{1-e^{-2\Gamma h}}{2\Gamma} \right\} \quad (16)$$

For a direct measurement with a vertical beam $\text{VAR}[\hat{w}_o] = \text{VAR}[v_r]/N$. If we require that, for our maximum height h_m , $\text{VAR}[\bar{w}] = \text{VAR}[\hat{w}_o]$, then the range can be found by solving

$$2\Gamma h_m = \ln \left\{ 1 + \frac{\Gamma h_m r^2}{2h_m^2} \left[1 - \frac{h_m^2}{r^2} \right] \frac{n}{N} \right\} \quad (17)$$

Because of the accuracy needed for vertical velocity estimates, the number N of vertical data will be much larger than the n - N data for horizontal wind component estimation. Thus in (17) we can assume $n/N=1$. Using $h_m = 10$ km, $\Gamma = 0.113 \text{ km}^{-1}$ in (17) gives $r \approx 40$ km, so $\theta_{em} \approx 14^\circ$. For heights lower than h_m , $\text{VAR}[\bar{w}]$ is less than for a direct measurement.

To compare the variances for direct and indirect measurements, assume that we have $n/10$ measurements at each level for estimating u_o , v_o , and w_o at each of 10 levels spaced 1 km apart. Solving (16) assuming a specified $\text{VAR}[\bar{w}] = 10^{-3} \text{ m}^2 \text{ s}^{-2}$ at $h_m = 10$ km with $\text{VAR}[v_r] = 1 \text{ m}^2 \text{ s}^{-2}$ gives $n = 1080$. So there are 108 data at each level and, from (8) $\text{VAR}[u_o] \approx 2 \times 10^{-2} \text{ m}^2 \text{ s}^{-2}$. With 108 data at each

level for the direct VAD measurement techniques, the $\text{VAR}[\hat{w}_0]$ is larger than that obtained using the indirect method even with $\theta_e = 90^\circ$. Because w_0 needs to be estimated with better accuracy than u_0, v_0 , consider that most measurements are made with a vertical beam. We need at least 4 data spaced 90° apart on a circle at each level in order to remove the bias in \hat{u}_0, \hat{v}_0 due to u_x, v_x (Equation 7). Thus from (8) we have $\text{VAR}[\hat{u}_0] \geq 0.5 \text{ m}^2 \text{ s}^{-2}$ which should be satisfactory for horizontal wind estimates but which is an order of magnitude larger than obtained by the indirect method. Furthermore, we have at most 104 data available at each level for the vertical beam with the consequence that $\text{VAR}[w_0] \approx 10^{-2} \text{ m}^2 \cdot \text{s}^{-2}$, an order of magnitude or more (at $h < 10 \text{ km}$) larger than obtained using the indirect method. A comparison of these variances is shown in Figure 11.

In reality, the variances for the indirect measurement technique may not be this much smaller, since we have neglected the dependence of signal strength (and $\text{VAR}[v_r]$) with range. However, this analysis has shown that the indirect technique does not require a tradeoff between vertical and horizontal variance. It offers the advantages of low variances, an areal averaged vertical velocity, and requires no assumption about the spatial structure of the wind to measure vertical velocity.

SUMMARY AND CONCLUSIONS

We have examined the errors in three radar techniques (three fixed beams, VAD, and VED) used to directly measure the three components of the wind. Equations were derived for the bias and variance of the uniform wind components estimates under the assumption of a spatially linear, time invariant wind field

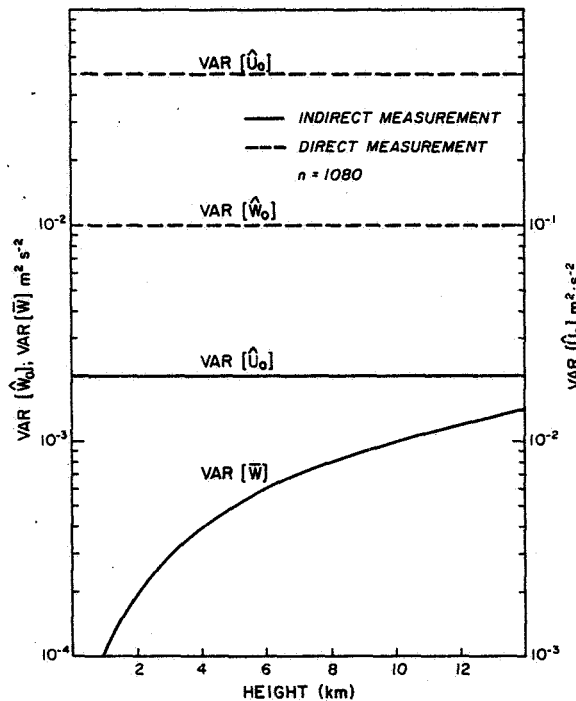


Figure 11. Comparison of wind estimate variances for direct and indirect techniques.

and a constant radial velocity measurement error. The measurement errors produce variance in the estimates and the linear wind shear biases the estimates. The variance of the estimates can be reduced by averaging more measurements but the biases cannot. Thus, for these direct measurement techniques, the selection of an elevation angle for simultaneous observation requires a compromise based on the required accuracy of the measurement.

We have also examined the errors for an indirect measurement technique based on Gauss's theorem with an equation of continuity constraint. Two advantages this indirect technique offers are that it does not require any assumptions about the spatial structure of the wind to measure vertical velocity and that its error variance can be smaller because it does not require a vertical and horizontal measurement variance compromise.

ACKNOWLEDGEMENTS

Our thanks to Joy Walton for her efficient preparation of the manuscript, to Joan Kimpel for drafting the figures, and to Robert Goldsmith for the photographic reductions.

REFERENCES

- Anton, H. (1981), Elementary Linear Algebra, John Wiley, 375 pp.
- Doviak, R. J. and D. S. Zrnic' (1983), Doppler Weather Radar and Weather Observations, Academic Press, New York (in press).
- Koscielny, A. J., R. J. Doviak and R. Rabin (1982), Statistical considerations in the estimation of divergence from single Doppler radar and application to pre-storm boundary layer observation, J. Appl. Meteor., 21, 197-210.
- Peterson, V. L. and B. B. Balsley (1979), Clear air Doppler radar measurements of the vertical component of wind velocity in the troposphere and stratosphere, Geophys. Res. Lett., 6, 933-946.
- Waldteufel, P. and H. Corbin (1979), On the analysis of single Doppler data, J. Appl. Meteor., 18, 532-542.
- Zrnic', D. S. (1979), Estimation of spectral moments for weather echoes, IEEE Trans. Geo. Elec., GE-17, 113-128.

APPENDIX 1. ANALYSIS OF THE FIXED BEAM TECHNIQUES

For the fixed beam technique with one vertical, and two off-vertical beams at elevation θ_e , azimuths 0° and 90° , we find, following the notations of KOSCIELNY et al. (1982), that

$$P_{nm} = \begin{bmatrix} \cos\theta_e & 0 & \sin\theta_e \\ \text{(repeats (n-N)/2 times)} & & \\ 0 & \cos\theta_e & \sin\theta_e \\ \text{(repeats (n-N)/2 times)} & & \\ 0 & 0 & 1 \\ \text{(repeats N times)} & & \end{bmatrix} = P_{n3}$$

$$P_{nm}^T P_{nm} = \begin{bmatrix} \frac{(n-N)}{2} \cos^2\theta_e & 0 & \frac{(n-N)}{2} \cos\theta_e \cdot \sin\theta_e \\ & \frac{(n-N)}{2} \cos^2\theta_e & \frac{(n-N)}{2} \cos\theta_e \cdot \sin\theta_e \\ & & N + (n-N) \sin^2\theta_e \end{bmatrix} \equiv P_3^T P_3$$

Since this is a symmetric matrix, we have not entered the identical terms below the diagonal elements. We invert $P_3^T P_3$ by performing a sequence of row operations to reduce it to the identity matrix. Performing this same sequence on the identity matrix reduces it to $[P_3^T P_3]^{-1}$ (ANTON, 1981). Thus

$$(P_3^T P_3)^{-1} = \begin{bmatrix} \frac{2\sec^2\theta_e}{n-N} + \frac{\tan^2\theta_e}{N} & \frac{\tan^2\theta_e}{N} & -\frac{\tan\theta_e}{N} \\ & \frac{2\sec^2\theta_e}{n-N} + \frac{\tan^2\theta_e}{N} & -\frac{\tan\theta_e}{N} \\ & & \frac{1}{N} \end{bmatrix} \quad (\text{A1.1})$$

For an equal number of measurements on each beam, $3N=n$ and

$$\text{VAR}(\hat{u}_o) = \text{VAR}(\hat{v}_o) = \frac{3\sigma_\epsilon^2}{n} (\sec^2\theta_e + \tan^2\theta_e) \quad (\text{A1.2})$$

$$\text{VAR}(\hat{w}_o) = \frac{3\sigma_\epsilon^2}{n} \quad (\text{A1.3})$$

The biasing of the estimates by the derivatives of the linear wind can be computed from the alias matrix of (3). Since the analysis is for constant height, all vertical derivatives cause no bias. Thus, for equal numbers of measurements,

$$P_{n\ell} = \begin{bmatrix} r \cos^2\theta_e & 0 & r \cos\theta_e \cdot \sin\theta_e & 0 \\ \vdots & \vdots & \vdots & \vdots \\ 0 & r \cos^2\theta_e & 0 & r \cos\theta_e \cdot \sin\theta_e \\ \vdots & \vdots & \vdots & \vdots \\ 0 & 0 & 0 & 0 \\ \vdots & \vdots & \vdots & \vdots \end{bmatrix}$$

$A_{34} = [P_{nm}^T P_{nm}]^{-1} P_{nm}^T P_{nl}$ and performing the multiplication gives

$$A_{34} = \begin{bmatrix} r \cos\theta_e & & r \sin\theta_e & \\ 0 & r \cos\theta_e & 0 & r \sin\theta_e \\ 0 & 0 & 0 & 0 \end{bmatrix}$$

Using the approximation $h = r \sin\theta_e$

$$A_{34} = \begin{bmatrix} h \cot\theta_e & 0 & h & 0 \\ 0 & h \cot\theta_e & 0 & h \\ 0 & 0 & 0 & 0 \end{bmatrix} \quad (A1.4)$$

and $K_l^T = [u_x, v_y, w_x, w_y]$.

For the fixed beam technique with three beams at elevation θ_e and azimuths 0° , 120° , and 240° , we find that

$$P_{nm} = \begin{bmatrix} \sin 0^\circ \cdot \cos\theta_e & \cos 0^\circ \cdot \cos\theta_e & \sin\theta_e \\ \vdots & \vdots & \vdots \\ \sin 120^\circ \cdot \cos\theta_e & \cos 120^\circ \cdot \cos\theta_e & \sin\theta_e \\ \vdots & \vdots & \vdots \\ \sin 240^\circ \cdot \cos\theta_e & \cos 240^\circ \cdot \cos\theta_e & \sin\theta_e \\ \vdots & \vdots & \vdots \end{bmatrix}$$

so

$$(P_{nm}^T P_{nm}) = \begin{bmatrix} \frac{n \cos^2\theta_e}{2} & 0 & 0 \\ 0 & \frac{n \cos^2\theta_e}{2} & 0 \\ 0 & 0 & n \sin^2\theta_e \end{bmatrix}$$

and

$$(P_{nm}^T P_{nm})^{-1} = \begin{bmatrix} \frac{2 \sec^2\theta_e}{n} & 0 & 0 \\ 0 & \frac{2 \sec^2\theta_e}{n} & 0 \\ 0 & 0 & \frac{\csc^2\theta_e}{n} \end{bmatrix} \quad (A1.5)$$

The alias matrix can be computed as before. For this case the predictor function for deformation is nonzero so

$$P_{nl} = \begin{bmatrix} 0 & 0 & r \cos^2 \theta_e & 0 & r \sin \theta_e \cdot \cos \theta_e \\ \vdots & \vdots & \vdots & \vdots & \vdots \\ -abr \cos^2 \theta_e & a^2 r \cos^2 \theta_e & b^2 r \cos^2 \theta_e & ar \cos \theta_e \cdot \sin \theta_e & -br \sin \theta_e \cdot \cos \theta_e \\ \vdots & \vdots & \vdots & \vdots & \vdots \\ abr \cos^2 \theta_e & a^2 r \cos^2 \theta_e & b^2 r \cos^2 \theta_e & -ar \cos \theta_e \cdot \sin \theta_e & -br \sin \theta_e \cdot \cos \theta_e \\ \vdots & \vdots & \vdots & \vdots & \vdots \end{bmatrix}$$

where $a = \sqrt{3/2}$ and $b = 1/2$. Computing A as before,

$$A_{35} \approx \begin{bmatrix} \frac{h \cot \theta_e}{2} & 0 & 0 & h & 0 \\ 0 & \frac{-h \cot \theta_e}{2} & 0 & 0 & \frac{h}{3} \\ 0 & \frac{h \cot^2 \theta_e}{2} & \frac{h \cot^2 \theta_e}{6} & 0 & \frac{h \cot \theta_e}{3} \end{bmatrix} \quad (A1.6)$$

and $K_l^T = [u_y + v_x, u_x, v_y, w_x, w_y]$.

APPENDIX 2. ANALYSIS OF THE VAD TECHNIQUES.

For the VAD technique, n radial velocity data are collected on a circle at height h . So

$$P_{nm} = \begin{bmatrix} \cos \theta_e \cdot \sin \phi_1 & \cos \theta_e \cdot \cos \phi_1 & \sin \theta_e \\ \cos \theta_e \cdot \sin \phi_2 & \cos \theta_e \cdot \cos \phi_2 & \sin \theta_e \\ \vdots & \vdots & \vdots \\ \cos \theta_e \cdot \sin \phi_n & \cos \theta_e \cdot \cos \phi_n & \sin \theta_e \end{bmatrix}$$

and

$$P_{nm}^T P_{nm} = \begin{bmatrix} \Sigma \cos^2 \theta_e \cdot \sin^2 \phi_i & \Sigma \cos^2 \theta_e \cdot \sin \phi_i \cos \phi_i & \Sigma \cos \theta_e \cdot \sin \theta_e \cdot \sin \phi_i \\ & \Sigma \cos^2 \theta_e \cdot \cos^2 \phi_i & \Sigma \cos \theta_e \cdot \sin \theta_e \cdot \cos \phi_i \\ & & \Sigma \sin^2 \theta_e \end{bmatrix}$$

where all summations are for $i=1, 2, \dots, n$. To simplify $P_{nm}^T P_{nm}$, we approximate the summations by integrals. For example,

$$\Sigma \cos^2 \theta_e \sin^2 \phi_i \approx \cos^2 \theta_e \frac{n}{2\pi} \int_{-\pi}^{\pi} \sin^2 \phi d\phi = \frac{n}{2} \cos^2 \theta_e.$$

A similar evaluation of the remaining summations gives

$$P_{nm}^T P_{nm} = \begin{bmatrix} \frac{n \cos^2 \theta_e}{2} & 0 & 0 \\ 0 & \frac{n}{2} \cos^2 \theta_e & 0 \\ 0 & 0 & n \sin^2 \theta_e \end{bmatrix}$$

Thus

$$(P_{nm}^T P_{nm})^{-1} = \begin{bmatrix} \frac{2 \sec^2 \theta_e}{n} & 0 & 0 \\ 0 & \frac{2 \sec^2 \theta_e}{n} & 0 \\ 0 & 0 & \frac{\csc^2 \theta_e}{n} \end{bmatrix}$$

and

$$\text{VAR}(\hat{u}_o) = \text{VAR}(\hat{v}_o) = \frac{\sigma_\epsilon^2}{h} 2 \sec^2 \theta_e \quad (\text{A2.1})$$

$$\text{VAR}(\hat{w}_o) = \frac{\sigma_\epsilon^2}{n} \csc^2 \theta_e \quad (\text{A2.2})$$

To find the bias caused by neglecting the parameters of a linear wind field, we compute the alias matrix where $K_5^T = [u_y + v_x, u_x, v_y, w_x, w_y]$. For analysis at constant height,

$$n\lambda = r \cos \theta_e \begin{bmatrix} \cos \theta_e \cdot \cos \phi_1 \cdot \sin \phi_1 & \cos \theta_e \cdot \sin \phi_1 & \cos \theta_e \cdot \cos \phi_1 & \sin \theta_e \cdot \sin \phi_1 & \sin \theta_e \cdot \cos \phi_1 \\ \cos \theta_e \cdot \cos \phi_2 \cdot \sin \phi_2 & \cos \theta_e \cdot \sin \phi_2 & \cos \theta_e \cdot \cos \phi_2 & \sin \theta_e \cdot \sin \phi_2 & \sin \theta_e \cdot \cos \phi_2 \\ \vdots & \vdots & \vdots & \vdots & \vdots \\ \cos \theta_e \cdot \cos \phi_n \cdot \sin \phi_n & \cos \theta_e \cdot \sin \phi_n & \cos \theta_e \cdot \cos \phi_n & \sin \theta_e \cdot \sin \phi_n & \sin \theta_e \cdot \cos \phi_n \end{bmatrix}$$

performing the matrix multiplications in (5), approximating summations by integrals, and using $h \approx r \sin \theta_e$ gives

$$A_{35} = \begin{bmatrix} 0 & 0 & 0 & h & 0 \\ 0 & 0 & 0 & 0 & h \\ 0 & \frac{h \cot^2 \theta_e}{2} & \frac{h \cot^2 \theta_e}{2} & 0 & 0 \end{bmatrix} \quad (\text{A2.3})$$

APPENDIX 3. ANALYSIS OF VED TECHNIQUE.

In the VED technique, the azimuth is fixed and the elevation angle is scanned. The range r is selected so the data are for a constant height h . To measure both horizontal components, another azimuth, preferably at 90° to the first, must be scanned. We assume $\frac{n}{2}$ data are collected for each scan. For convenience, we introduce the horizontal distance s which is directed along the azimuth ϕ . We make estimates of a horizontal component u_o (directed along s) and the vertical component w_o . The predictor function matrix is

$$P_{nm} = \begin{bmatrix} \cos\theta_1 & \sin\theta_1 \\ \cos\theta_2 & \sin\theta_2 \\ \vdots & \vdots \\ \cos\theta_n & \sin\theta_n \end{bmatrix}$$

so

$$P_{nm}^T P_{nm} = \begin{bmatrix} \sum \cos^2\theta_i & \sum \cos\theta_i \cdot \sin\theta_i \\ \sum \sin^2\theta_i & \end{bmatrix}$$

where the summations are for $i=1, 2, \dots, \frac{n}{2}$ and θ_i is the elevation angle. Approximating the summations by integrals,

$$\sum \cos^2\theta_i \approx \frac{n}{2(\pi-2\theta_o)} \int_{\theta_o}^{\pi-\theta_o} \cos^2\theta d\theta = \frac{n}{4} \left[\frac{(\pi-2\theta_o) - \sin 2\theta_o}{\pi-2\theta_o} \right]$$

$$\sum \sin\theta_i \cos\theta_i \approx 0$$

$$\sum \sin^2\theta_i \approx \frac{n}{4} \left[\frac{(\pi-2\theta_o) + \sin 2\theta_o}{\pi-2\theta_o} \right]$$

so

$$(P_{nm}^T P_{nm})^{-1} = \begin{bmatrix} \frac{4}{n} \left[\frac{(\pi-2\theta_o)}{(\pi-2\theta_o) - \sin 2\theta_o} \right] & 0 \\ 0 & \frac{4}{n} \left[\frac{(\pi-2\theta_o)}{(\pi-2\theta_o) + \sin 2\theta_o} \right] \end{bmatrix}$$

and

$$\text{VAR}(\hat{u}_o) = \text{VAR}(\hat{v}_o) = \frac{\sigma_\epsilon^2}{n} 4 \left[\frac{\pi-2\theta_o}{(\pi-2\theta_o) - \sin 2\theta_o} \right]$$

$$\text{VAR}(\hat{w}_o) = \frac{\sigma_\epsilon^2}{n} 2 \left[\frac{\pi-2\theta_o}{(\pi-2\theta_o) + \sin 2\theta_o} \right]$$

(A3.1)

The variance of w_o is halved since we assume the results from the two scans will be averaged.

The bias by the linear terms is again computed by the alias matrix. The prediction functions corresponding to the excluded parameters are

$$P_{nl} = \begin{bmatrix} r \cos^2 \theta_1 & r \sin \theta_1 \cdot \cos \theta_1 \\ r \cos^2 \theta_2 & r \sin \theta_2 \cdot \cos \theta_2 \\ \vdots & \vdots \\ r \cos^2 \theta_n & r \sin \theta_n \cdot \cos \theta_n \end{bmatrix}$$

Performing the matrix multiplications, approximating summation by integrals and using $h \approx r \sin \theta$ gives

$$A_{22} = \begin{bmatrix} 0 & h \\ h \begin{bmatrix} (\pi - 2\theta_o) - \sin 2\theta_o \\ (\pi - 2\theta_o) + \sin 2\theta_o \end{bmatrix} & 0 \end{bmatrix}$$

For the combined analysis of two scans at 0° and 90° ,

$$A_{34} = \begin{bmatrix} 0 & 0 & h & 0 \\ 0 & 0 & 0 & h \\ h \begin{bmatrix} (\pi - 2\theta_o) - \sin 2\theta_o \\ (\pi - 2\theta_o) + \sin 2\theta_o \end{bmatrix} & h \begin{bmatrix} (\pi - 2\theta_o) - \sin 2\theta_o \\ (\pi - 2\theta_o) + \sin 2\theta_o \end{bmatrix} & 0 & 0 \end{bmatrix}$$

and the vector of excluded parameters is

$$K_4^T = (u_x, v_y, w_x, w_y).$$